Paper No.
48-SA-30

Paper No.

CAVITATION CHARACTERISTICS AND INFINITE ASPECT RATIO CHARACTERISTICS OF A HYDROFOIL SECTION

James W. Daily,
Assistant Professor of Hydraulics,
Massachusetts Institute of Technology.
Formerly Hydraulic Engineer at the Hydrodynamics Laboratory
of the California Institute of Technology

Advance Copy
Released for publication upon presentation

Contributed by the Hydraulic Division for presentation at the Semi-Annual Meeting, Milwaukee, Wis., May 30-June 4, 1948, of The American Society of Mechanical Engineers.

Paper No. 521-K-48

CAVITATION CHARACTERISTICS AND INFINITE ASPECT RATIO CHARACTERISTICS OF A HYDROFOIL SECTION

ABSTRACT

This paper describes "two-dimensional" tests in a water tunnel of a profile identical to the 4412 airfoil section of the National Advisory Committee for Aeronautics. The tests included photographic observations of the inception and growth of cavitation as influenced by velocity, pressure (submergence) and angle of attack, and measurements, during cavitation-free operation, of the hydrodynamic forces and moments as functions of Reynolds number and angle of attack. The relation between the angle of attack and the value of the cavitation parameter at which inception occurs is shown for each face of the hydrofoil. The effect of profile geometry in causing cavitation, and the significance of distinctly different types of cavitation obtained with change in variables are discussed. Convenient curves are given showing the submergence required to avoid cavitation for different velocities and angles of attack. The measured hydrodynamic characteristics are presented in graphical form and are also compared with previously existing data from wind tunnel tests of a finite aspect ratio span. The experimental procedure and its reliability in indicating true infinite aspect ratio characteristics is discussed.

INTRODUCTION

The usefulness of a profile as a hydrofoil depends upon its susceptibility to cavitation and its behavior when cavitating, as well as its hydrodynamic characteristics when cavitation is absent. In the past the bulk of the basic hydrofoil performance data has been determined either in wind tunnels where cavitation can not be produced, or in towing tanks where cavitation, if produced, cannot be examined conveniently. Therefore, not only have there been very little data available showing the cavitation characteristics of hydrofoil shapes, but there have been only a few very limited descriptions of how cavitation begins and grows on a hydrofoil surface.

In 1943 a test program was undertaken in the High Speed Water Tunnel of the California Institute of Technology (1) which provided an opportunity for making a detailed study of the characteristics of a hydrofoil that included cavitation as well as the normal hydrodynamic data. This program was initiated at the request of the David Taylor Model Basin with the objective of investigating in general the testing of small scale hydrofoils in a water tunnel of the Cal-Tech type under both cavitating and non-cavitating conditions.

For these experiments, the test installation in the water tunnel was arranged to provide as nearly as practical two-dimensional flow so that all observations and measurements would correspond to the infinite aspect ratio condition. The actual investigations included:

1. Visual and photographic observations of the cavitation on the hydrofoil as it appeared, developed, and disappeared, as functions of both velocity and angle of attack.

2. Measurements of the hydrodynamic forces and moments acting on the hydrofoil, also as functions of velocity and angle of attack. For reasons to be discussed the force measurements were limited to the non-cavitating conditions. The results of both categories of tests are presented here, together with a discussion of the test procedures used.

(1) Numbers in parentheses refer to references at end of paper.

EXPERIMENTAL EQUIPMENT AND INSTALLATION

The Hydrofoil Profile

Test units with profiles identical to the N.A.C.A. 4412 airfoil section were supplied for these experiments by the David Taylor Model Basin. The profile of this section is shown in Figure 1, together with a tabulation of its coordinates. It is one of the four digit series shapes of the National Advisory Committee for Aeronautics described in references (2), (3), (4), and (5). It has a 12 per cent thickness ratio with a 4 per cent camber. The hydrodynamic characteristics, including surface pressure measurements, had been determined previously by wind tunnel tests and were available for comparing with the water tunnel data.

The Water Tunnel

A diagram showing the Cal-Tech water tunnel (1) as it was when used for these experiments is given in Figure 2.* The tunnel is a closed circuit type with an enclosed jet working section. The absence of any free surface limits experiments to those simulating conditions at great depths. In this tunnel water is circulated (counter clockwise in Figure 2) with a variable speed pump to give a wide range of velocities in the cylindrical working section. The working section diameter is 14-inches and its length is 72-inches. Visual and photographic observations can be made through transparent lucite windows whose inner faces conform to the cylindrical shape of the tunnel. A system of pressure regulation permits the fluid pressure in the working section to be controlled independently of the velocity, so that cavitation can be produced or avoided as desired. The tunnel is equipped with a three component balance for measuring the hydrodynamic forces and moments acting on a test body. The balance system is shown schematically in Figure 3. A rigid vertical spindle is supported near its mid point in such a way that it is free to rotate about any axis but cannot translate. One end projects into the working section to receive the test unit on which certain hydrodynamic forces and moments act. The other end is restrained from moving by the application of external forces and couples. By measuring the magnitudes of the restraining forces the corresponding hydrodynamic forces acting on the test unit are obtained. In this balance the restraining forces are created by hydraulic pressure acting on a piston and cylinder assembly. The pressure, which is measured by precision weighing type pressure gages, is proportional to the force applied. Provisions are incorporated in the spindle structure for rotating the upper portion of the spindle about its own geometric axis so that the angle of attack of the test unit can be changed during tests.

Test Installation

Since the so-called infinite aspect ratio characteristics were desired in these experiments, two-dimensional flow was approximated by having the test unit completely span the working section. In this instance the circular cross section of the stream was modified by inserting panels at top and bottom of the working section to form parallel walls as shown in Figure 4. In the approximately rectangular section which resulted, the test unit was mounted spanwise between the two plane walls. This type of installation causes approximately a uniform effect of the hydrofoil on the fluid along the full length of the test span. The span was

*For a description of the High Speed Water Tunnel as recently revised see "The Hydrodynamics Laboratory at the California Institute of Technology", by R. T. Knapp, Joseph Levy, J. Pat O'Neill, and F. Barton Brown, Trans. A.S.M.E., vol. 70, 1948.

supported at one tip by the balance spindle and cantilevered into the stream. The hydrofoil angle of attack was changed by rotating the spindle. Referring to Figure 1, a positive angle signified a clockwise rotation of the hydrofoil. Measurements of drag, lift, and pitching moment were obtained as reactions of the pressure cylinders shown in Figure 3.

In addition to the desirability of having a large span to chord ratio, the proportions of the hydrofoil test unit depended upon the physical capacity of the balance and force measuring apparatus, and the structural rigidity of the test unit itself. In order to remain within the capacity range of the balance it was necessary to reduce the size of the test until, and hence its rigidity in the lift direction. Thus, if the cantilevered hydrofoil completely spanned the working section, severe deflections were obtained at high lifts. As a result two installations were provided as shown in Figure 5. In one the test unit spanned the entire 10-inch distance between top and bottom walls except for small clearance gaps at either end. In the other the test unit spanned one half the 10-inch space up to the centerline of the tunnel. A dummy section extending from top down comprised the remainder of the span. A small gap at the lower wall and at the center line of the tunnel between the ends of the two semispans served to isolate the lower half during measurements. An angle indexing device permitted the angle of attack of the upper half to be changed simultaneously with the lower. With this arrangement the forces transmitted to the balance were cut in half, permitting an extension of the range of test velocities. Furthermore, the maximum deflection of the hydrofoil for any particular velocity and angle of attack was reduced by a large factor. With the 3-inch chord dimension finally selected as a compromise between the several factors, it was possible to obtain measurements for Reynolds numbers of nearly 1,000,000. The 3-inch size resulted in a good chord to span ratio (3.33) and was also large enough to permit an accurate shaping of the profile. Figure 6 is a photograph of the two semispans used, and Figure 7 is a view into the end of the working section, showing the parallel walls and the test unit in place.

CAVITATION CHARACTERISTICS

Definition of Cavitation

The word "cavitation" is used to signify either the hydrodynamic phenomenon of the formation of vapor filled bubbles or "cavities" at low pressures and the subsequent collapse of such bubbles, or the physical damage to materials that form the boundaries of the fluid passages in which this bubble formation and collapse occurs. In this article attention is limited to the phenomenon itself. By this usage, an object such as a projectile, a hydrofoil, or a pump blade is said to "cavitate" if such vapor bubbles are formed, even though no physical damage occurs.

It is generally assumed that cavitation will occur whenever the pressure at some point in the fluid becomes equal to the vapor pressure. Local "boiling" results in vapor filled "cavities" which grow so long as they are in a low pressure environment, but collapse when carried by the relative flow into a zone of high pressure. Assuming the beginning or "inception" of cavitation occurs when the pressure equals the vapor pressure exactly, implies that the fluid will not support a tension and ignores the possibility of dissolved gasses being released to cause premature cavitation at pressures higher than the vapor pressure. Nevertheless, there is considerable experimental information to indicate that with water containing ordinary amounts of impurities and dissolved air, cavitation does occur at pressures that are very close to the vapor pressure.

The Cavitation Parameter

A relative flow between an immersed object and the surrounding fluid results in a variation in pressure along the surface of the object. At any point on the object the difference between the pressure at that point and the pressure in the undisturbed fluid at some distance from the object is proportional to the square of the relative velocity, or

$$\frac{P_o - P}{\rho \frac{V_o^2}{2}} = \text{constant}$$

where P_o and V_o are the pressure and velocity for the undisturbed fluid, P is the pressure at the surface of the object, and ρ is the density of the fluid. At some point on the object P will be a minimum and $\frac{P_o - P_{min}}{\rho \frac{V_o^2}{2}}$ will have a definite value. In the absence of cavitation (and neglecting Reynolds Number effects) this value will depend only upon the shape of the object. Now it is easy to imagine a set of conditions such that P_{min} becomes equal to the vapor pressure of the liquid. This could be accomplished by increasing the relative velocity V_o for a fixed value of the pressure P_o, or by continuously lowering P_o with V_o held constant. Either procedure will result in a lowering of the absolute values of all the local pressures on the surface of the object. If carried to the point that P_{min} equals the vapor pressure, incipient conditions are said to exist and cavitation should begin.

This beginning will mean the appearance of tiny cavities at or near the place on the object where the minimum pressure is obtained. If a pressure less than the vapor pressure is not possible (which is assumed) then continual increase in V_o (or decrease in P_o) will mean that the pressure at other points along the surface of the object will become equal to the vapor pressure. Thus the zone of cavitation will extend from its original inception point.

Up to the inception point the value of the fraction $\frac{P_o - P_{min}}{\rho \frac{V_o^2}{2}}$ remains fixed. For conditions beyond the inception point the value decreases since P_{min} is identically equal to the vapor pressure, whereas V_o is increasing (or P_o is decreasing). Thus the value of this fraction becomes an index of the stage of advancement or "degree" of cavitation.

Written with the vapor pressure replacing P_{min}, thus

$$\frac{P_o - P_{vp}}{\rho \frac{V_o^2}{2}} = K$$

this fraction can be used as a cavitation parameter to relate the conditions of flow to the possibility of cavitation occurring, as well as to the degree of cavitation once the phenomenon begins. Thus, for any system where the relative

velocity is V_o and the pressure in the fluid is P_o, K will have a definite value. Cavitation will occur only if the shape of the immersed object is such that

$$\frac{P_o - P_{min}}{\rho \frac{V_o^2}{2}} \geq K$$

For the particular case of $\frac{P_o - P_{min}}{\rho \frac{V_o^2}{2}} = \frac{P_o - P_{vp}}{\rho \frac{V_o^2}{2}} = K$

the value is known as K_i (K for inception of cavitation) on the particular object.

By adjusting the flow conditions so K is greater than, equal to, or less than K_i, the full range of possibilities can be established from no cavitation to advanced stages of cavitation.

The immersed object referred to in the above discussion can be actually a body such as a hydrofoil, or the solid boundary of the passage such as the throat of a Venturi meter.

Test Procedure

The procedure used during cavitation tests was to vary the pressure while all the other factors were held constant. Thus, for a given angle of attack, α_o, at any velocity the pressure was reduced in steps until cavitation appeared and then became well developed, that is until K became equal to, and then, less than K_i. The cavitation parameter for each step was calculated from simultaneously measured values of the velocity and pressure. Measurements were taken as α_o was varied from -10^o to $+16^o$. Flow velocities, ranged up to 45 feet per second. During these experiments the inception and development of cavitation was photographed through the transparent windows. These photographs were made with high voltage flash lamps having a flash duration of about 20 microseconds.

Inception of Cavitation vs. Angle-of-Attack

In Figure 8 the value of the cavitation parameter at which cavitation first appears on the hydrofoil is plotted as a function of the angle of attack. Two curves are shown, one marking the incipient cavitation on the hydrofoil's upper surface and one on its lower. In the area above the curves cavitation did not occur, while below the curves it existed in varying degrees. These two curves cross at $\alpha_o = -1.4^o$ where cavitation appeared simultaneously on top and bottom surfaces. For any other angle cavitation occurred on one surface before the other.

Furthermore, the lowest value of K at which cavitation appeared is at -1.40^o. As already mentioned the inception point depends upon the shape of the object presented to the flow. Figure 1 shows that with the chord of the foil (line joining leading and trailing edges) parallel to the flow, the upper surface will cause a greater deflection of fluid, higher local velocity, and should cause a lower pressure than will the lower surface. Figure 8 indicates that this is true. For $\alpha_o = 0^o$ cavitation was visible first on the upper side at K = 0.7 and later on the lower side at K = 0.42. As the hydrofoil was pitched into the stream, with either positive or negative angles, the flow had to pass around the sharply curved leading edge. This resulted in increased accelerations and lower pressures

so that cavitation occurred earlier (at higher K values). The lowest pressure was on the lower surface of the hydrofoil if α_o was negative, but on the upper surface if α_o was positive. As α_o was changed from zero the surface which was pitched into the stream was subjected to extra dynamic pressure. At first this merely delayed cavitation on this surface, but eventually the pressure became so large that cavitation did not occur on this side at all. Thus, for example, for positive angles, cavitation was not obtained on the underside of the foil for angles greater than about 2 1/2°.

K_i from Wind Tunnel Pressure Distribution Data

If the distribution of static pressure over the surface of a body is known for non-cavitating flow, the fraction

$$\frac{P_o - P_{min}}{\rho \frac{V_o^2}{2}} = K_i$$

can be evaluated. Pressure distribution measurements have been made in the wind tunnel for the NACA 4412 airfoil (3), and values of K_i calculated from this data are compared in Figure 8 with the values obtained in the water tunnel.

Good agreement is shown for the upper side of the hydrofoil up to an angle of about 7°. Beyond this, K_i as predicted from the wind tunnel is higher than the water tunnel values. Similarly for the lower surface best agreement is shown near zero angle, with increasing deviation at large negative angles. Several factors are of possible importance in explaining the discrepancies. First, at attack angles away from zero the sharply curved leading edge of the hydrofoil is presented to the flow. Small errors in formation of the profile here will result in large errors in the minimum pressures. In fact, this indicates that extreme care must be taken in the manufacture of models, particularly small scale ones, if accurate and consistent results are to be expected. The second factor is that for both the wind tunnel and the water tunnel the greatest deviations from infinite aspect ratio conditions are at large angles of attack. The effect of the proximity of the walls (particularly those parallel to the hydrofoil's pitching axis) becomes a singificant variable (6). One further possibility is that ordinary water will support a tension under dynamic loading, despite impurities and turbulence. If this is so, a cavity will not form unless the fluid is subjected to the low pressure environment for a definite length of time. With a sudden drop and sharp rise in pressure, such as the flow experiences as it passes over the leading edge of the hydrofoil at large angles of attack, the fluid may pass through the low pressure zone before a cavity develops. Thus, the first cavitation would appear only at reduced values of K where the low pressure zone is extended. This latter question is one of the important unanswered questions about the mechanics of cavitation.

Submergence to Prevent Cavitation

In many applications of hydrofoils the static pressure is measured in terms of submergence, the vertical depth of the unit below the water surface. The data of Figure 8 has been replotted in Figure 15 to show the submergence necessary to prevent completely cavitation on the hydrofoil. The submergence is given in the left hand diagram as a function of velocity for certain angles of attack and in the right hand diagram as a function of angle of attack for fixed velocities. In each of the two diagrams all points below the constant α_o or constant V_o curves are for cavitation-free operation. Note that the minimum submergence is required when $\alpha_o = -1.4°$; for all other angles it is greater. Note also that at a given velocity the range of

angles is limited. For example, at 70 feet per second and 30 feet submergence cavitation-free operation is possible only within the limits of -2.2° and $+2.4^{\circ}$.

It should be emphasized that the method of obtaining these data corresponds to conditions expected at appreciable depths below the free surface. If the hydrofoil is but slightly submerged there results a production of waves at the surface and a change in the relative flow pattern near the hydrofoil itself. This will change the values of K_i for the hydrofoil and hence the accuracy of the data for shallow submergences in the two diagrams of Figure 15.

The Zone of Cavitation

The behavior of a cavitating hydrofoil depends upon how the cavitation forms and grows and how these cavities affect the flow. In Figures 10 to 14 inclusive, are shown the appearance of cavitation on one or both surfaces of the hydrofoil at several stages of development. Each figure is for a fixed attack angle and velocity of flow. The variation in K and hence degree of cavitation was obtained by changing the pressure in the working section. (The semispan installation was in use when these photographs were taken and the horizontal joint marking the division between the two halves can be seen in some cases.) Figure 9, which will be useful in discussing these photographs, is another diagram of K_i vs α_o on which have been indicated numbers corresponding to the several photographs in Figures 10 to 14. Each number is located on the diagram at the value of K and at the angle of attack at which its photograph was taken. Thus the relationship between conditions for inception of cavitation and the conditions for each photograph is shown graphically.

The relative susceptibility to cavitation on the two surfaces of the hydrofoil is shown in the photographs in Figure 11, which were taken with zero angle of attack. In 11a, b, c, in the left hand column are views of cavitation on the lower (normally high pressure) surface of the hydrofoil. For these views the relative flow over the surface is from right to left. In 11d, e, f, g in the right hand column cavitation is shown on the upper surface. The relative flow is from left to right. Reference now to Figure 9 shows that cavitation first appears on the upper surface at $K = 0.7$, approximately, for $\alpha_o = 0^{\circ}$. Cavitation does not appear on the lower surface until K is reduced to about 0.41. In Figure 11 the first photograph for the upper surface is at $K = 0.57$. Even at this value cavitation does not occur over the entire length of the span continuously, but rather intermittently in any one local area. Other photographs taken at the same K would show patches of cavitation in other positions along the span. As K is reduced, cavitation becomes more general and more extended. In the meantime cavitation on the lower surface shows a less advanced stage compared to that on the upper at approximately the same K values. Thus at $K = 0.37$ cavitation on the lower surface is very little more general than on the upper at $K = 0.57$. In fact the relative degree of cavitation is shown clearly in Figure 11a where tail wisps of cavitation on the upper side can be seen extending past the trailing edge.

Similar observations are obtained from Figure 13 and 14, for $\alpha_o = +8$ and $+12^{\circ}$, except that in both these cases no cavitation appears on the lower surface for the range of the experiments. The pitch is such that the extra dynamic pressure prevents vaporization on this side. On the other hand, at $\alpha_o = -4^{\circ}$ the upper surface, which was pitched into the stream, was cavitation free.

As K is reduced, cavitation first appears as a narrow zone of small cavities which apparently originate, grow, and finally collapse on or near the surface of the hydrofoil. In the early stages, at least, the extent of the zone of cavities is an indication of the extent of the low pressure zone, an idea that has been substantiated for certain three dimensional bodies (13). A clean example of

such an expanding low pressure zone is shown in Figures 10a, b, c.

The determination of the location and extent of the low pressure zone by water tunnel tests such as these has an important application in the development of high speed airfoils. The occurrence of cavitation at the minimum pressure point with liquids is analogous to the occurrence of sonic velocities and shock waves at the minimum pressure point with compressible fluids.

Advanced Stages and the Entrainment Process

With continued reduction in K a stage is reached where the collapse actually occurs in the fluid downstream from the hydrofoil itself. In fact, there exists a growing tendency for groups of cavities to be separated from the general mass and carried well beyond the hydrofoil and the main zone of cavitation before collapsing. Examples of this are shown in Figures 10c and 14e, f. Professor Knapp has pointed out that this is an "entrainment" process whereby the main flow of fluid is acting as an entrainment pump. It is an essential feature in the mechanics of maintaining the pressure at the boiling point for the advanced stages of cavitation. For extremely advanced stages apparently the bulk of the vapor is entrained and swept away before collapsing.

Under some conditions the individual cavities in the very advanced stages of cavitation coalesce to form a single enveloping bubble with transparent walls over a portion of its length. One example is in Figure 10d, where such a transparent bubble envelopes the near side of the hydrofoil. In Figures 11c and 11g the flow is on the verge of changing over to this transparent bubble condition. The transparent walls are an indication that very little vaporization is occurring. The vapor supply must be from the zone of turbulent boiling near the downstream end of the envelope. The interior of the envelope is at the vapor pressure and is maintained at this pressure by the "pumping" action of the relative flow past the hydrofoil.

Fine vs. Coarse Grain Cavitation

A general examination of the photographs shows two "types" of cavitation to exist. In one, such as shown in Figure 12, individually identifiable cavities appear. In the other, such as in Figures 10 or 13, the cavities are very small and closely spaced, giving a sudsy appearance. Professor Knapp has termed these "coarse grain" and "fine grain", respectively. It will be noted that these types are associated with the curvature of the profile presented to the flow. A sharp curvature with its sudden reduction in pressure results in the fine grain type. With a more gentle curvature the coarse grain bubbles appear. These photographs show that as the hydrofoil is given larger and larger angles of attack in either direction the minimum pressure point moves toward the sharply curved leading edge and fine grain cavitation is produced.

Rate of Growth and Life of a Cavity

In many of the photographs the growth of individual cavities can be observed for a short distance after their formation. Some measurements made for $\alpha_o = 0^o$, $V_o = 45$ feet per second, and $K = 0.25$ showed a rapid growth, for the first quarter chord length of travel, up to 60% to 75% of what appeared to be the final diameter. Beyond this, growth was considerably slower until individual cavities interfered with their neighbors and then lost their identity. The growth of the cavities probably is the result of the continued vaporization into the "void" until the cavity itself is swept into a higher pressure zone. For an example of the rapidity of the process, the life of the cavities shown in Figure 11e is approximately 1/200 seconds. In this short interval the cavity grows to a diameter of

approximately 5/16" and then collapses.

Hydrodynamic Behavior with Cavitation

These photographs show instantaneous samples of an unsteady phenomenon. The average or so-called "steady state" condition obtained for a given K value represents a balance between the rate of vapor formation and the rate of annihilation, whether the latter is by collapse as in the early stages or by entrainment as in the later stages. For any K the extent of the cavitation zone grows until this balance is obtained. Successive samples at the same velocity and pressure will have the same general appearance, but will differ in detail. This unsteady character results in fluctuating hydrodynamic forces on the hydrofoil, the well known cause of the vibration of cavitating ships' propellers or centrifugal pumps. With increased cavitation these fluctuating forces (and hence vibrations of the hydrofoil) were observed to grow to dangerous magnitudes. However, with the formation of the transparent enveloping bubble mentioned above the forces became essentially steady and the vibrations nearly ceased. Under these conditions, apparently the fluctuations associated with cavity formation and collapse were limited to the neighborhood of the cavities themselves and not carried back upstream to the hydrofoil proper.

The hydrodynamic forces and moments acting during cavitation were not measured during these experiments for two related reasons. First, the water tunnel balance, which was designed for essentially steady force measurements, would not resolve the unsteady forces encountered with cavitation over most of the range of the studies. Second, it was observed, by noting the deflections of the hydrofoil unit, that even though the drag increased with the onset of cavitation, the lift (and pitching moment) dropped off. Low average values combined with fluctuating forces further complicated measurements of these. The effect of cavitation on the hydrodynamic behavior of the hydrofoil depends on the extent to which the cavitation alters the flow around the unit. The existence of cavitation means that the streamlines must conform to the shape of a new "body" and that the velocity and pressure distribution is changed from that without cavitation. As the cavitation zone grows, less and less fluid is given a net deflection normal to the direction of motion and the lift drops off. This effect is similar to that encountered when airfoils stall at excessive angles of attack. At the same time the drag goes up because cavitation increases the effective thickness of the body, resulting in a larger change in momentum of the fluid parallel to the flow direction.

Cavitation and Damage

While these experiments were not concerned with cavitation damage, it might be noted that it is the initial stages of cavitation that are probably responsible for cavitation erosion. In the early stages the cavity collapse takes place on or near the hydrofoil surface. At later stages the collapse is in the liquid body well away from the solid surface. Since it is generally recognized that it is the collapse that results in damage, it must be the early stages that are dangerous. This is an important consideration in dealing with propellers and pumps which often operate near the conditions for incipient cavitation.

Significance of this Profile

This cavitation data is presented principally as a study of the cavitation process in the inception, growth and collapse of cavities or bubbles. The use of this particular profile for the experiments was convenient because of the existence of the previously measured wind tunnel data. Otherwise this shape has no particular merit as a hydrofoil so far as cavitation is concerned. Other shapes exist which are far more "resistant" to the occurrence of cavitation. However, their other

hydrodynamic characteristics are also different from those for this shape. In the selection of a profile for an application the requirements of both types of characteristics must be considered.

INFINITE ASPECT RATIO CHARACTERISTICS

Significance of Infinite Aspect Ratio Data

The hydrodynamic properties of airfoil and hydrofoil shapes are reported as "infinite aspect ratio" or "section" characteristics because in this form, they depend only on the shape of the profile. The characteristics of a hydrofoil or airfoil of finite span differ from those for an infinite span because of "leakage" of fluid at the span tips from the high pressure to low pressure surface. This flow around the ends acts to reduce the lift and increase the drag at given angles of attack. These are called "induced" effects (7) (8) and their magnitude depends on the aspect ratio, plan form, and twist of the particular hydrofoil. Infinite aspect ratio data is important in the design of lifting devices, such as wings, rudders, or stabilizing fins, as well as various pumping devices such as propellers, fans and centrifugal pumps. Methods are available for converting this data to the equivalent performance of actual devices having arbitrary geometrical proportions, (8) (9) (10).

Experimental Methods

Infinite aspect ratio data can be obtained from tests of finite span sections by correcting the measured forces and moments for induced velocity effects and for tunnel wall interference and support interference effects. In an effort to eliminate the uncertainty of the various corrections, which may become large with respect to the measured forces, particularly drag, the trend has been towards two-dimensional tests. In these the attempt is made to cause the hydrofoil to act uniformly along its space as it deflects the passing fluid by having the test unit span the stream completely. If this is achieved, the resulting flow differs from the ideal sought only by the effect of the presence of the tunnel walls.

As already described, the test installation for these experiments was designed to give essentially two dimensional flow past the hydrofoil. The clearance gaps at the ends of the test span, which were necessary to isolate the unit while measuring forces, were small to make the tip "leakage" unimportant.

The hydrodynamic forces acting on a hydrofoil need not be measured directly but may be determined indirectly by evaluating the change in momentum of the fluid as it passes the test span and by measuring the reaction pressures created on the tunnel walls as a result of the fluid being deflected. These wake survey and wall pressure survey methods (11) (12) require less elaborate test equipment because the force measuring balance is eliminated and the test unit need not be supported independently of the tunnel structure as is necessary for direct measurement of the forces acting on the hydrofoil. On the other hand, where the balance is available, its use for direct measurements is extremely convenient and, with the proper provisions, should permit better accuracy. One objective of this study was to investigate the adaptation of the single spindle three component balance to two dimensional testing.

Measured Characteristics

The measured data was obtained over the range of Reynolds number from R = 287,000 to 903,000. The experimental procedure was to measure the lift, drag, and pitching moment as functions of the angle of attack for the several Reynolds numbers. In each case the pressure was maintained high enough to prevent cavitation.

The experimental results are shown graphically in Figures 16 and 17, where lift, drag and pitching moment coefficients, and center of pressure are plotted versus angle of attack. In Figure 18 angle of attack and drag and pitching moment coefficients are plotted with lift coefficient considered as the independent variable. The terms and symbols used are defined in Table III at the end of this paper. In each Figure curves are given for four values of Reynolds number. All the results plotted here were obtained with the split span installation which permitted the measurement of the forces on one half the total span. Even so, it will be noted that the maximum lift could not be reached at the higher Reynolds numbers because of the excessive magnitude of the forces developed. Measurements with the full 10 inch span, which were in the lower Reynolds number range, gave similar results to those shown and are not included here. In Table I the magnitudes of the important variables for both the semispan and full span installations are listed for each Reynolds number.

As Reynolds number increases certain consistent changes in performance will be noted. The slope of the lift coefficient curve and the maximum value of the lift coefficient increase, while the drag coefficient decreases. Also the angle for zero lift shifts to slightly lower values. The moment coefficient is figured about the aerodynamic center, the point about which the pitching moment is essentially constant for a wide range of angles of attack. Up to about 5° the coefficient is constant and independent of Reynolds number. Up to 8° the coefficient is within 15% of a constant value. The center of pressure is also nearly independent of R, with deviations occurring near $\alpha_o = 0^{\circ}$ where accuracy in calculating the center of pressure position is low.

Experimental Limitations on Results

The experimental arrangement used for these tests introduced the following three factors causing deviation of the flow from truly two-dimensional conditions:

1. The entire span was not subject to a uniform velocity, but experienced lower velocities in the boundary layer zone near the tunnel walls.

2. There was the possibility of flow through the clearance spaces between the ends of the test span and the tunnel walls or between the two halves of the split span section.

3. There was a possibility of interference because of the proximity of the tunnel walls to the test section.

A non-uniform velocity distribution will tend to make all the coefficients numerically high. However, as shown in Figure 4, the test span was located only about one tunnel diameter from the final contraction of the flow. In this short distance the boundary layer should occupy only a small percentage of the width of the working section so that most of the span should experience the full velocity. It should be noted also that while the velocity distribution was known to be uniform in the circular section just ahead of the final contraction caused by the addition of the two parallel walls to the working section, it was not measured in the plane of Section AA (Figure 4) where the hydrofoil was mounted. Good evidence of uniformity at the hydrofoil was obtained from an examination of the cavitation photographs. In these, cavitation appeared to form at the same value of K_i at all points along the span and grow uniformly along the span, with no consistent deviations. (The intermittent patches of cavitation in the early stages as shown in some cases are thought to be evidence of the unsteady nature of the phenomenon.

Any leakage through the clearance spaces at the ends of the test span will tend to reduce the actual angle of attack at the hydrofoil at high lifts. In these tests the clearance was held to 0.005" to keep a high resistance to flow through the gap. At small angles of attack the influence on the measured forces and moments should be small. However, as the angle increases and the pressure difference through the gap increases, the leakage will increase. This is an error that could be reduced by using end plates recessed into the tunnel wall, but these in turn would complicate the drag measurements. The magnitude of the clearance gap is important. Increasing the gap from 0.005" to 0.023" caused an 8% increase in drag and a 4% decrease in lift. The moment was not affected appreciably. If it is assumed that the error is proportional to the leakage and, therefore, for laminar flow, is proportional to the clearance, the maximum error in drag is about 2% with a 0.005" gap. It is likely that the error increases at a faster rate as the clearance is enlarged, so the error at 0.005" is even less. The error in lift from this cause is correspondingly less.

The tunnel walls confine the water flow and change the streamline pattern around the hydrofoil from that in a free stream. For two dimensional flow it is particularly important that the walls parallel to the pitching axis are as far removed as possible. In this installation the maximum dimension of the water tunnel cross section normal to the hydrofoil axis was kept at the full 14" as shown in Figure 4. Wall interference, including the so called "blocking" or actual restriction of the passage by the hydrofoil itself, is negligible at small angles of attack (low lifts) but increases with angle (6). The actual magnitude of this effect was not evaluated for these tests. The degree of fluid turbulence in the water tunnel was not determined because suitable instruments were not available for measuring it directly, as can be done readily with the hot wire anemometer in the wind tunnel, and because indirect measurements, such as the determination of the critical Reynolds number for a sphere, required test setups involving uncertain support interference errors. The turbulence has an important effect on the measured drag and maximum lift. Without more definite knowledge of the turbulence, measurements of these two items must be considered primarily as comparative.

Accurate measurement of the minimum drag was handicapped by the very small magnitudes of this component (approximately four pounds total for R = 903,000). Nevertheless, the decreasing trend with increasing Reynolds number already noted is in the proper direction and is a good indication that the tests give reliable comparative results.

In summary, it appears that with this method of testing accurate results should be obtained at small angles of attack. This is in the low lift range and the range of many hydrofoil applications. At larger angles the accuracy of the results is reduced somewhat. Nevertheless, good comparative results should be obtainable.

Theoretical Characteristics

A simple set of equations for the Characteristics of hydrofoils in a frictionless fluid can be derived theoretically by the method of conformal transformation (8). Using the Joukowsky transformation, the relationships for small angles of attack are:

$$\text{Lift coefficient} = c_{l_o}$$

$$= 2\pi \left(1 + 0.77 \frac{\text{thickness}}{\text{chord}}\right) \left(\frac{\alpha_o - \alpha_{l_o}}{57.3}\right)$$

Zero lift angle $= \alpha_{l_o}$

$$= 2 \frac{\text{camber}}{\text{chord}} \times 57.3$$

Slope of lift curve $= a_o$

$$= 2\pi \left(1 + 0.77 \frac{\text{thickness}}{\text{chord}}\right) \frac{1}{57.3}$$

Pitching moment coefficient $= c_{m_{a.c.}}$

$$= \frac{\pi}{2} \left(1 + 0.77 \frac{\text{thickness}}{\text{chord}}\right) \frac{\alpha_{l_o}}{57.3}$$

It will be noted that for a given thickness ratio the lift coefficient is proportional to the angle of attack, the angle for zero lift is proportional to the amount of camber, and the moment coefficient is constant about the quarter chord point. It will also be noted that because a frictionless fluid is assumed, all of these values are independent of Reynolds number and the drag is zero.

For the 4412 hydrofoil the numerical values are:

$$c_{l_o} = 0.120 \ (\alpha_o - \alpha_{l_o})$$

$$\alpha_{l_o} = -4.6^\circ$$

$$a_o = 0.120 \text{ (per degree)}$$

$$c_{m_{a.c.}} = -0.137$$

These values appear also in Table I where they are seen to be slightly greater (numerically) than the measured quantities.

Comparison with Finite Aspect Ratio Tests

Previously published data for this profile were obtained from N.A.C.A. tests of wing section with aspect ratio of six. The data were corrected to give infinite aspect ratio characteristics. In Figure 19 curves from N.A.C.A. wind tunnel tests are compared with the water tunnel measurements. The principal characteristics are tabulated in Table II. These wind tunnel data were taken from Reference (4), Figure 7, and corrected by the methods outlined on pages 17 and 18 of that reference, to give so-called "second approximation" characteristics. They apply at the test Reynolds numbers. All corrections to infinite aspect ratio are included except the effect of support interference on drag and certain secondary effects of variations in c_l and c_{d_o} along the finite test span at high lifts. They are not corrected for turbulence or scale effects and should not be confused with final characteristics presented in references (4) and (5) which have been extrapolated to full scale aircraft flight Reynolds numbers.

When comparing the two sets of data from different sources the fact should be kept in mind that most likely different degrees of turbulence existed in the two tunnels. As already noted, this factor would affect the drag and magnitude of the maximum lift attainable. The other characteristics should not be

affected appreciably. In this case the water tunnel two-dimensional tests gave ten per cent lower values for the slope of the lift curve, the moment coefficient, and the minimum drag coefficient. On the other hand, the maximum lift coefficient was higher in the water tunnel. The drag curves for the two sets of data differ widely in spite of the reasonable agreement of the minimum drag values. The reason for this discrepancy is not known.

Application of Results

In testing with artificial fluid streams the degree of turbulence is invariably different from that encountered in the actual application. The higher the turbulence, the higher will be the maximum lift coefficient. The turbulence also affects the transition in the boundary layer on a given body and hence the drag. Methods have been suggested for compensating for tunnel turbulence. These have their main value in adjusting the maximum lift coefficient.

The range of Reynolds number covered by the tests (up to approximately 1,000,000) includes many hydrofoil applications. If the data are to be applied outside this range, some correction should be made. Wind tunnel tests have shown that for Reynolds numbers up to 3,000,000 the slope of the lift curve increases only about one or two per cent above its value at 1,000,000. The pitching moment and the angle for zero lift are also nearly unaffected. On the other hand, the maximum lift coefficient increases from ten to twenty per cent. The profile drag decreases at nearly the same rate as turbulent skin friction on flat plates. It is felt that the useful range of these test results can be extended considerably by careful application of rules such as these.

It should be emphasized again that the data applies to situations where there is no free surface in the neighborhood of the hydrofoil. For operation at an inappreciable submergence the formation of waves on the liquid surface will modify the characteristics measured by tests such as these.

ACKNOWLEDGEMENT

This paper presents the results of an investigation conducted at the High Speed Water Tunnel of the Hydrodynamics Laboratory at the California Institute of Technology. The High Speed Water Tunnel was built and operated by the California Institute of Technology under Contract OEMsr-207 with the Office of Scientific Research and Development. Division 6, Section 6.1 of the National Defense Research Committee was the sponsoring agent of the OSRD during the establishment and initial four-year operating period of the Water Tunnel. The Hydrodynamics Laboratory and the Water Tunnel research program are under the immediate direction of Robert T. Knapp, Associate Professor of Hydraulic Engineering.

These experiments were made as a part of a general program of hydraulic investigations made for the armed services during the period of NDRC sponsorship. This particular investigation was made on request from the United States Navy Department, the David Taylor Model Basin, and on authorization from Dr. E. H. Colpitts, chief of Section 6.1 of the NDRC. The material included here originally appeared in Report No. 6.1-sr207-1273 submitted to the NDRC of the OSRD.

In the design of the two-dimensional test installation described here, helpful suggestions were obtained from Professor Theodore von Karman of the California Institute. Mr. Robert E. Carr, who was in charge of the water tunnel test crew, was responsible for execution of actual tests. The excellence of the large quantity of photographic is due to the efforts of Mr. Hugh Stevens Bell of the Water Tunnel staff. Mr. Haskell Shapiro was responsible for the lighting and miscellaneous electronic equipment auxiliary to the experimental set-up.

TABLE I

PRINCIPAL SECTION CHARACTERISTICS OF THE NACA 4412 HYDROFOIL
FROM TWO-DIMENSIONAL TESTS IN WATER TUNNEL

	Test Reynolds Number	Attack Angle for no lift α_{l_o} (deg)	Lift Curve Slope a_o (per deg)	Max. Lift Coefficient $c_{l_{max}}$	Min. Drag Coefficient $c_{d_{o\ min}}$	Pitching Moment $c_{m_{a.c.}}$	Aerodynamic Center Ahead of c/4 (% c)	Aerodynamic Center Above Chord (% c)
Semispan Installation	287,000	-3.95	0.098	1.36	0.014	-0.102	5.47	-0.26
	563,000	-4.05	0.102	1.39	0.013	-0.101	4.92	-4.52
	730,000	-4.15	0.104		0.0105	-0.102	5.53	-3.84
	903,000	-4.25	0.106		0.011	-0.101	5.39	1.68
Full-span Installation	299,000	-4 (approx)*	0.098	1.38	0.014	-0.100	5.12	-0.38
	388,000	-4 (approx)*	0.101		0.014	-0.102	5.12	-0.39
Theoretical Values for Infinite Aspect Ratio		-4.58	0.120			-0.137	0	0

*These values for α_{l_o} are obtained after correction for error in initial alignment of hydrofoil chord with tunnel axis

TABLE II

PRINCIPAL SECTION CHARACTERISTICS OF THE NACA HYDROFOIL
FROM WIND TUNNEL TESTS OF RECTANGULAR AIRFOILS
WITH ASPECT RATIO = SIX*

Test Reynolds Number	Attack Angle for no lift α_{l_o} (deg)	Lift Curve Slope a_o (per deg)	Max. Lift Coefficient $c_{l_{max}}$	Min. Drag Coefficient $c_{d_{o\ min}}$	Pitching Moment $c_{m_{a.c.}}$	Aerodynamic Center Ahead of c/4 (% c)	Aerodynamic Center Above Chord (% c)
331,000	-4.35	0.094	1.27	0.011	-0.096	1.1	-8.0
638,000	-4.25	0.094	1.36	0.012	-0.094	1.0	-1.0

*Wind Tunnel data were taken from Figure 7, Reference 4, and corrected by the methods outlined on Pages 17 and 18 of that reference to give so-called "second approximation" characteristics.

TABLE III

DEFINITIONS OF TERMS AND SYMBOLS

α_o = angle of attack between hydrofoil and mean flow of water in degrees

d_o = drag force per unit length of hydrofoil span in pounds

l_o = lift force per unit length of hydrofoil span in pounds

$m_{a.c.}$ = pitching moment per unit length of hydrofoil span in foot pounds, measured about the aerodynamic center

v_o = relative velocity between the water and the hydrofoil in feet per second

ρ = density of water in slugs per cubic foot

μ = absolute viscosity of water in pound seconds per square foot

c = chord of hydrofoil section in feet

b = span of hydrofoil test unit in feet

b/c = aspect ratio

a.c. = aerodynamic center, the point about which the pitching moment coefficient is independent of the angle of attack or lift coefficient

C.P. = center of pressure, the point at which the resultant of all the hydrodynamic forces acting on the hydrofoil is applied

Section Drag Coefficient

$$c_{d_o} = \frac{d_o}{\rho \frac{v_o^2}{2} c}$$

Section Lift Coefficient

$$c_{l_o} = \frac{l_o}{\rho \frac{v_o^2}{2} c}$$

Section Moment Coefficient (about aerodynamic center)

$$c_{m_{a.c.}} = \frac{m_{a.c.}}{\rho \frac{v_o^2}{2} c^2}$$

TABLE III (Continued)

Reynolds Number

$$R = \frac{v\, c\, \rho}{\mu}$$

Cavitation Parameter

$$K = \frac{P_o - P_{vp}}{\rho \frac{v_o^2}{2}}$$

Where in addition to terms defined above

P_o = absolute pressure in the undisturbed flow in pounds per square foot

P_{vp} = pressure in the cavitation bubble (taken as equal to the vapor pressure of water for these tests) in pounds per square foot

References

1. "The Water Tunnel as a Tool in Hydraulic Research", by James W. Daily, Proceedings of the Third Hydraulics Conference (1946), University of Iowa. Studies in Engineering, Bul. No. 31, pp. 169-91.

2. "The Characteristics of 78 Related Airfoil Sections from Tests in the Variable Density Wind Tunnel", by E. N. Jacobs, K. E. Ward and R. M. Pinkerton, N.A.C.A. T.R. No. 460, 1933.

3. "Calculated and Measured Pressure Distributions over the Midspan Section of the N.A.C.A. 4412 Airfoil", by R. M. Pinkerton, N.A.C.A. T.R. No. 563, 1936.

4. "Airfoil Section Characteristics as Affected by Variations of the Reynolds Number", by E. N. Jacobs and A. Sherman, N.A.C.A. T.R. No. 586, 1937.

5. "Airfoil Section Data Obtained in the NACA Variable-Sensity Tunnel as Affected by Support Interference and Other Corrections", by E. N. Jacobs and I. H. Abbot, N.A.C.A. T.R. No. 669, 1939.

6. "An Investigation of Fluid Flow in Two Dimensions", by A. Thom, A.R.C. Reports and Memoranda No. 1194, Nov. 1928.

7. "Aerodynamics of the Airplane", by C. B. Millikan, Wiley, New York, 1941, pp. 39-54.

8. "Aerodynamic Theory", Vol. II, edited by W. F. Durand, Julius Springer, Berlin, 1934.

9. "Determination of the Characteristics of Tapered Wings", by R. F. Anderson, N.A.C.A. T.R. No. 572, 1936.

10. "The Design of Propeller Pumps and Fans", by M. P. O'Brien and R.G. Folsom, Univ. of Calif. Public. in Engineering, Vol. 4, No. 1, University of California Press, 1939.

11. "The Measurement of Profile Drag by the Pitot Traverse Method", by B. M. Jones, A.R.C. Reports and Memoranda, No. 1688, 1936.

12. "The Effects of Roughness at High Reynolds Numbers on the Lift and Drag Characteristics of Three Thick Airfoils", by Frank T. Abbott, Jr. and Harold R. Turner, Jr., N.A.C.A. Wartime Report L-46. (Wake survey and wall pressure techniques were used for the two-dimensional tests described in this report.)

13. "Pressure Distribution and Cavitation on Submerged Boundaries", by John S. McNown, Proceedings of the Third Hydraulic Conference (1946), University of Iowa. Studies in Engineering, Bul. No. 31, pp. 192-208.

List of Figures

Station	Upper	Lower	Station	Upper	Lower
0	-	0	40.	9.80	-1.80
1.25	2.44	-1.43	50.	9.19	-1.40
2.5	3.39	-1.95	60.	8.14	-1.00
5.0	4.73	-2.49	70.	6.69	-0.65
7.5	5.76	-2.74	80.	4.89	-0.39
10.	6.59	-2.86	90.	2.71	-0.22
15.	7.89	-2.88	95.	1.47	-0.16
20.	8.80	-2.74	100.	0.13	-0.13
25.	9.41	-2.50	100.	-	0
30.	9.76	-2.26			

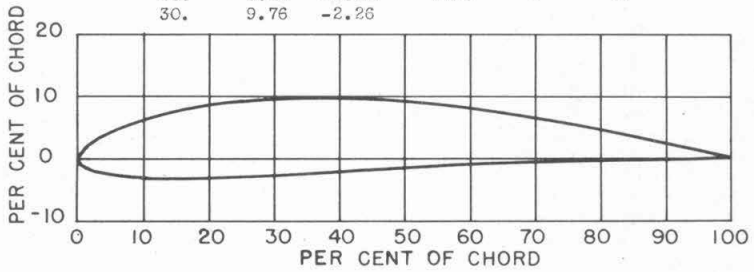

Leading edge radius 1.58
Slope of radius through end of chord 4/20
Maximum mean camber = 0.04 x chord
Location of maximum camber = 0.4 x chord
Maximum thickness = 0.12 x chord

Fig. 1.
Dimensions of N.A.C.A. 4412 Hydrofoil

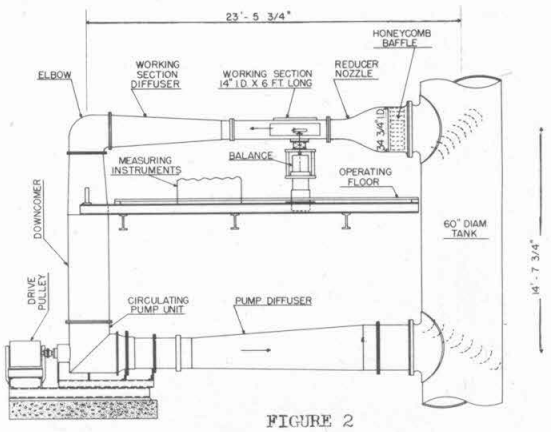

FIGURE 2

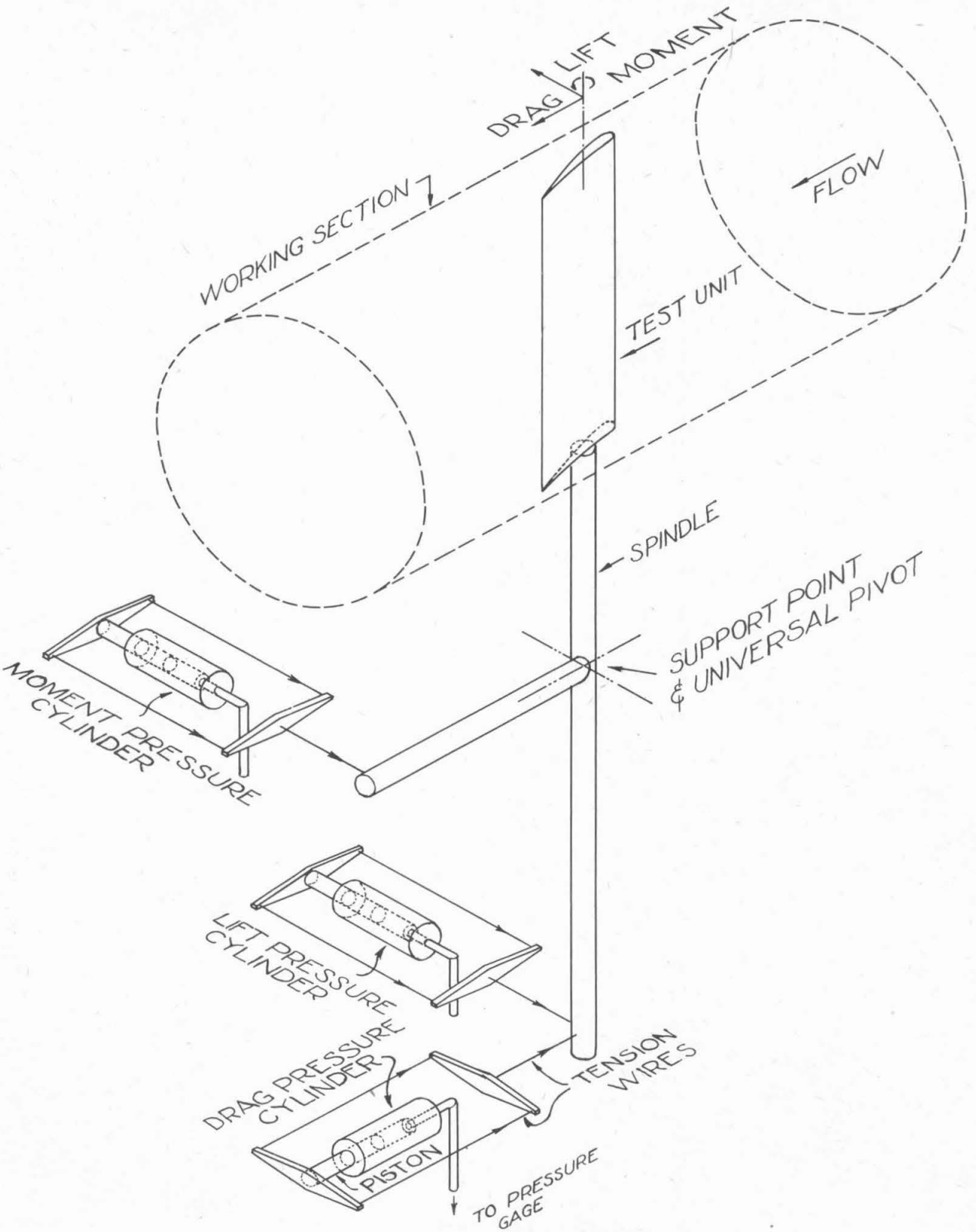
LIFT
DRAG
MOMENT
WORKING SECTION
FLOW
TEST UNIT
SPINDLE
SUPPORT POINT
& UNIVERSAL PIVOT
MOMENT PRESSURE CYLINDER
LIFT PRESSURE CYLINDER
DRAG PRESSURE CYLINDER
TENSION WIRES
PISTON
TO PRESSURE GAGE

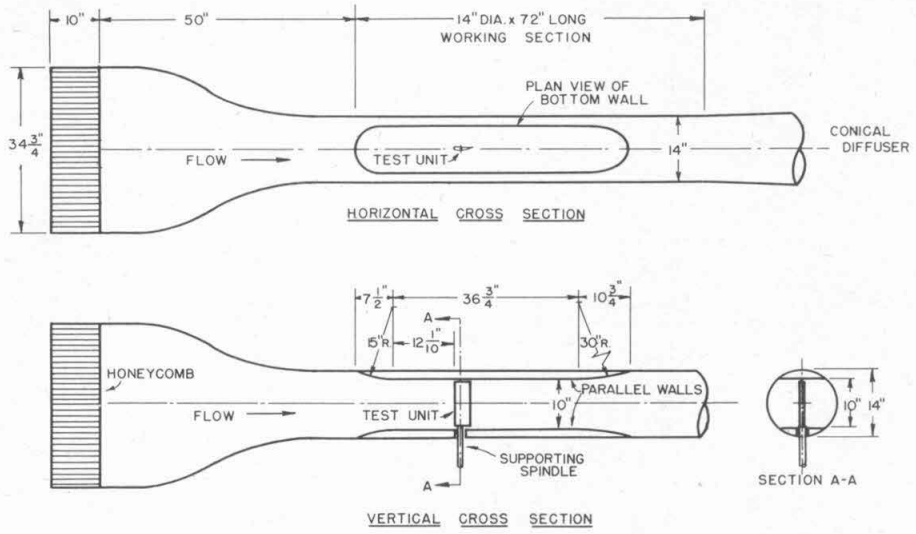

Fig. 4.

Hydrofoil Test Installation

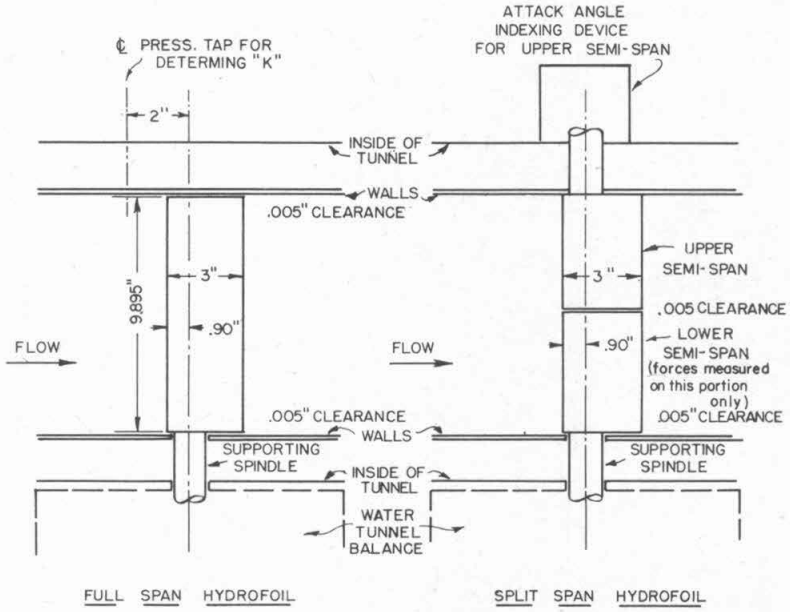

Fig. 5.

Details of Test Units

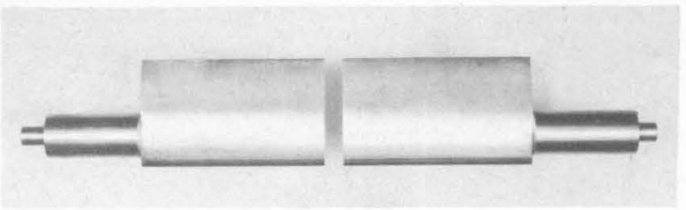

FIGURE 6

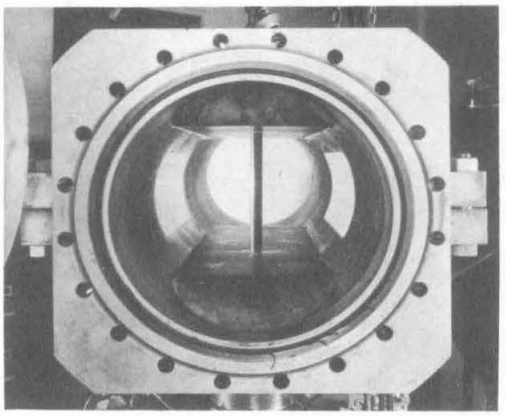

FIGURE 7

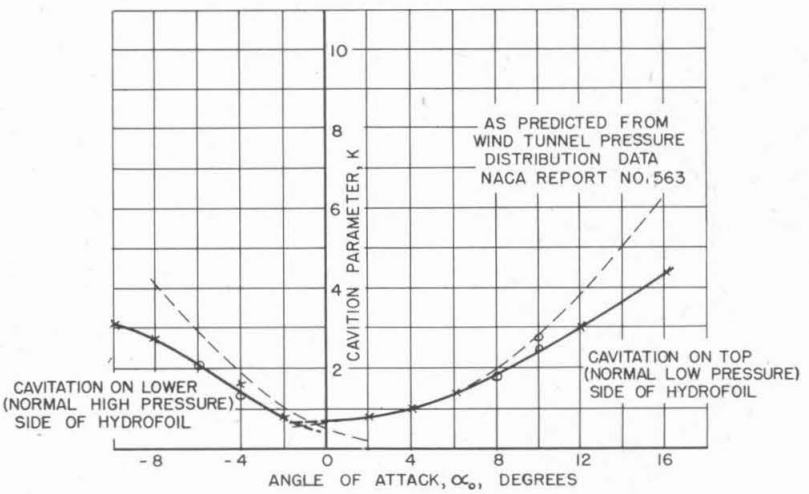

Fig. 8.

Values of "K_i" at which Cavitation Begins vs. Angle of Attack

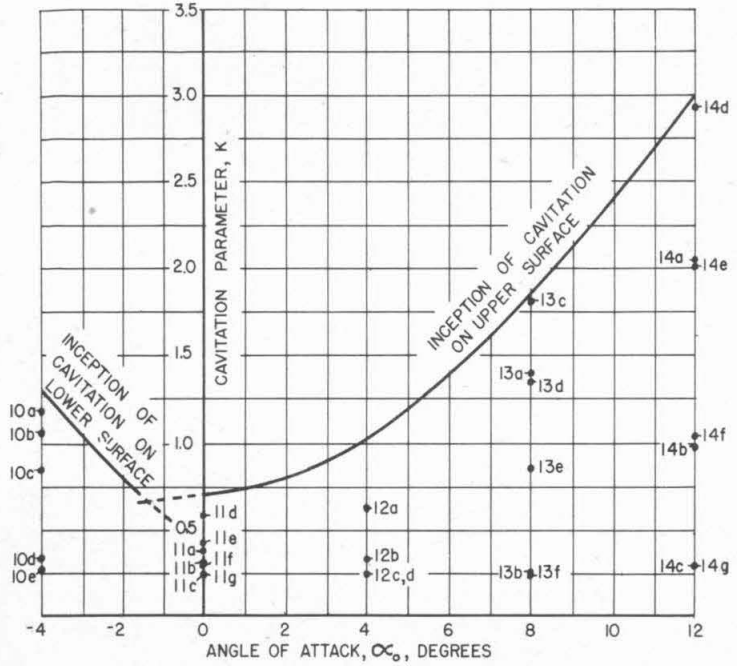

Fig. 9.

Diagram Showing Cavitation Test Conditions
for Each Photograph in Figures 10 to 14 inclusive

$\alpha = -4°$

V = 45 FT/SEC

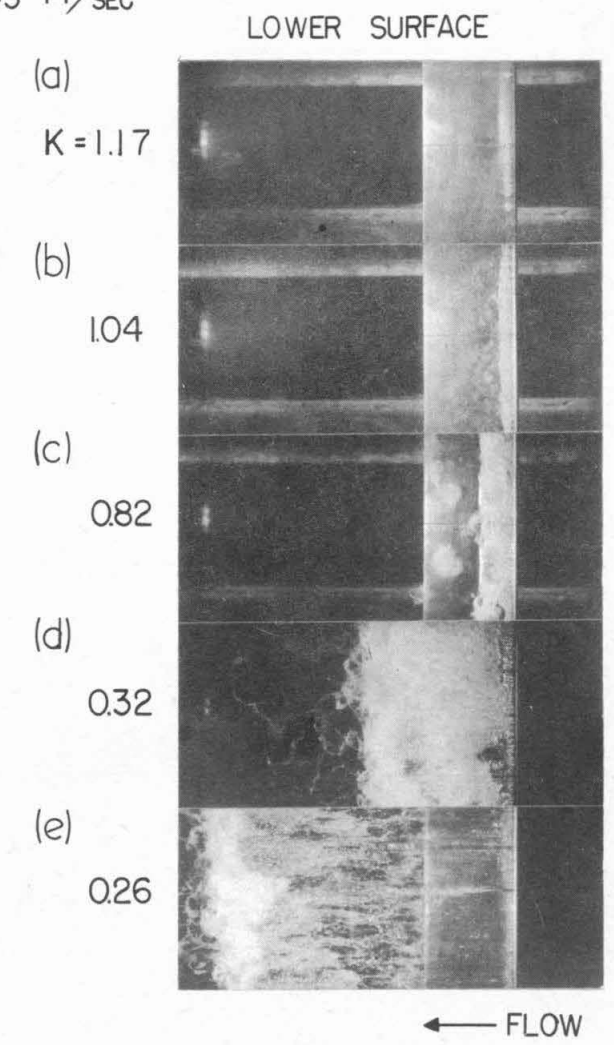

NACA 4412

J.W. DALY Fig 10

J. W. DAILY FIG. 11

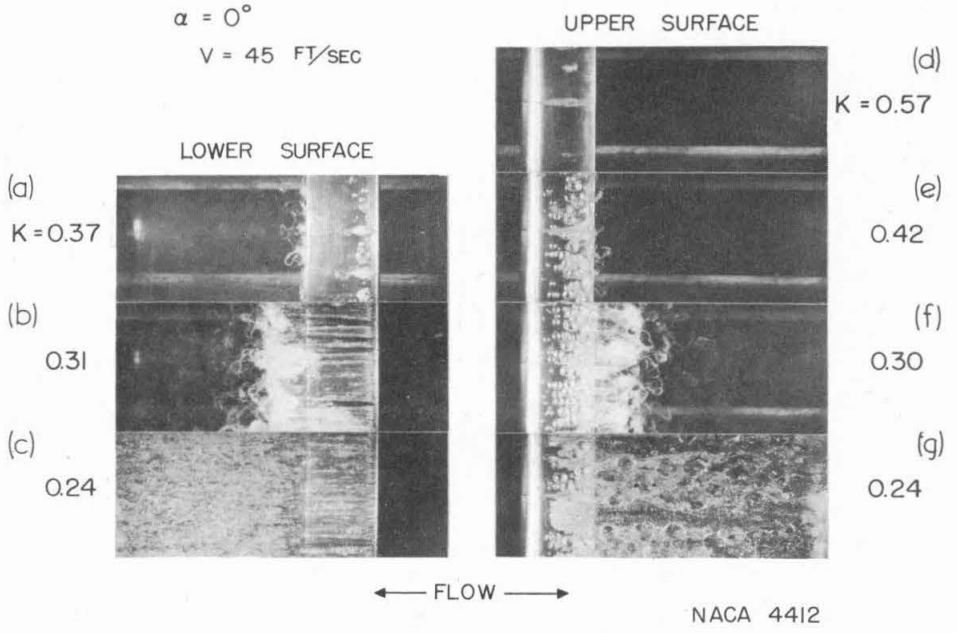

NACA 4412

J. W. DAILY FIG. 12

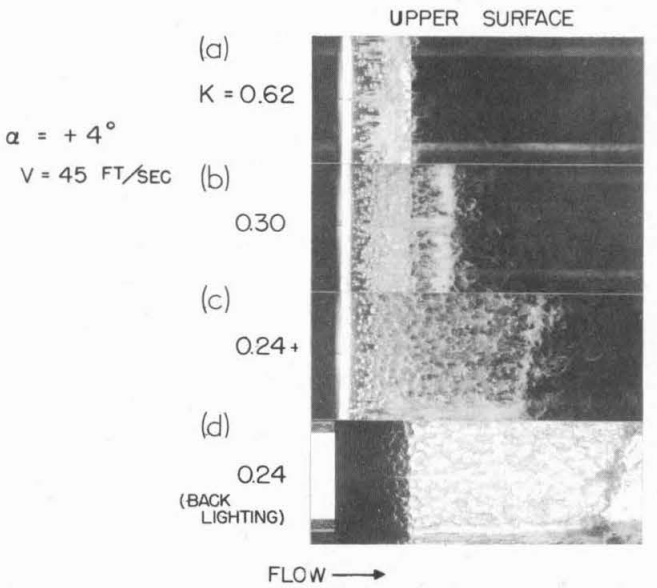

NACA 4412

J. W. DAILY FIG. 13

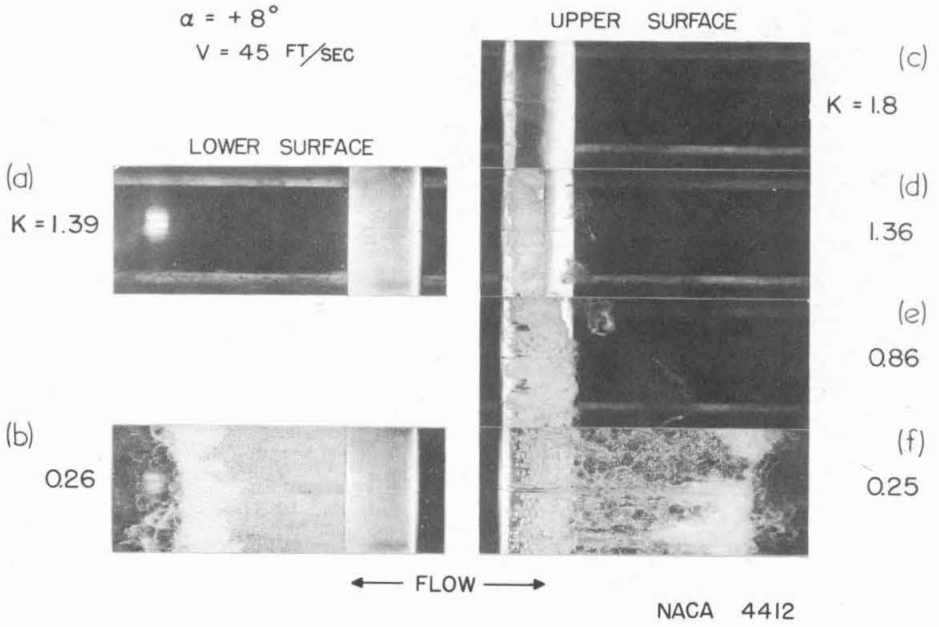

J. W. DAILY FIG. 14

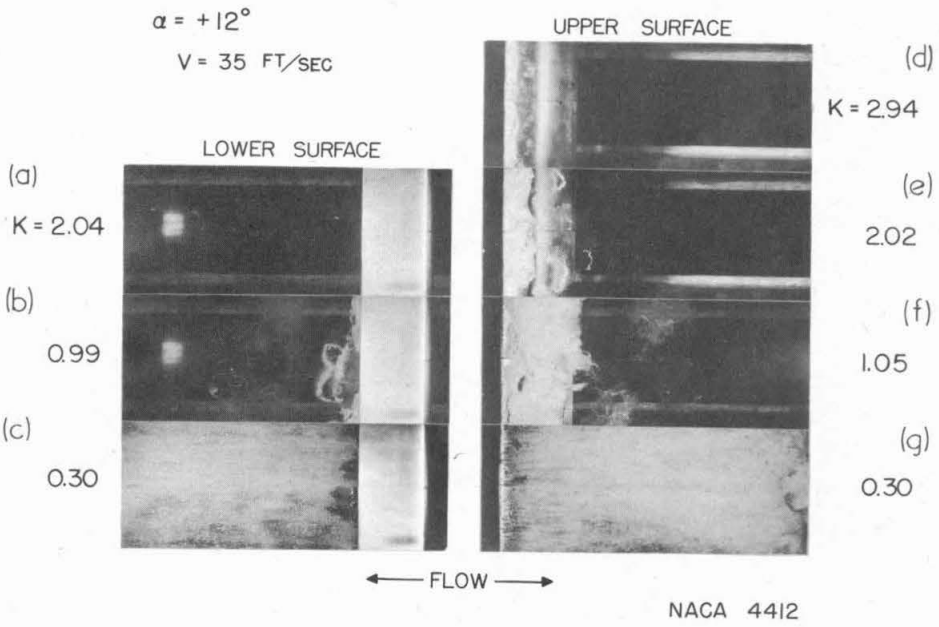

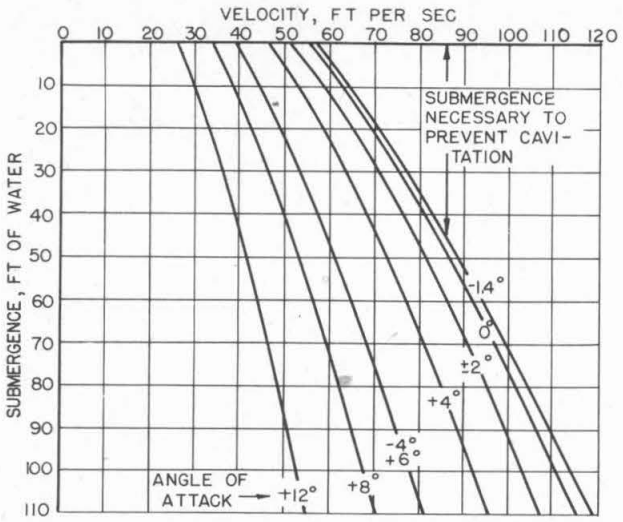

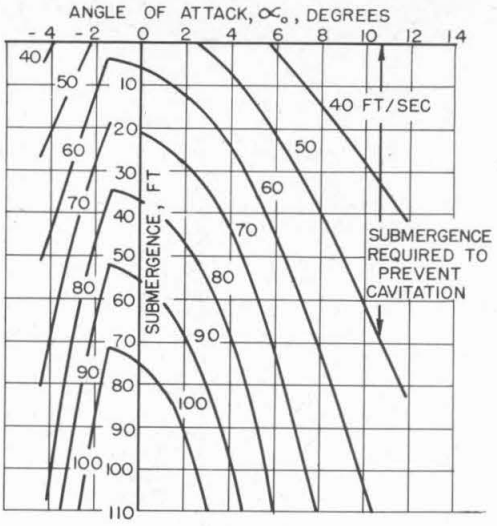

Fig. 15.

Submergence Necessary to Prevent Cavitation on Hydrofoil

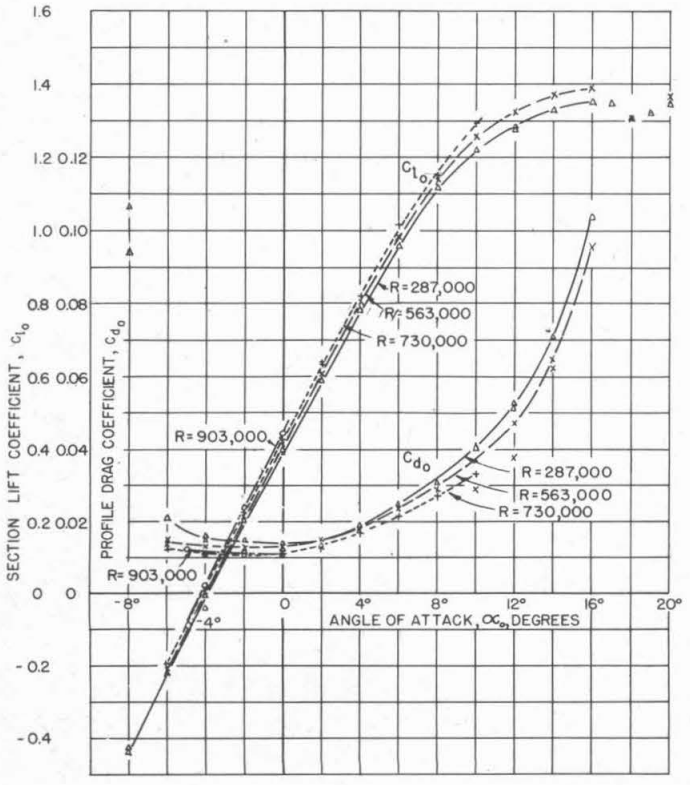

Fig. 16.

Infinite Aspect Ratio Characteristics vs. Angle of Attack

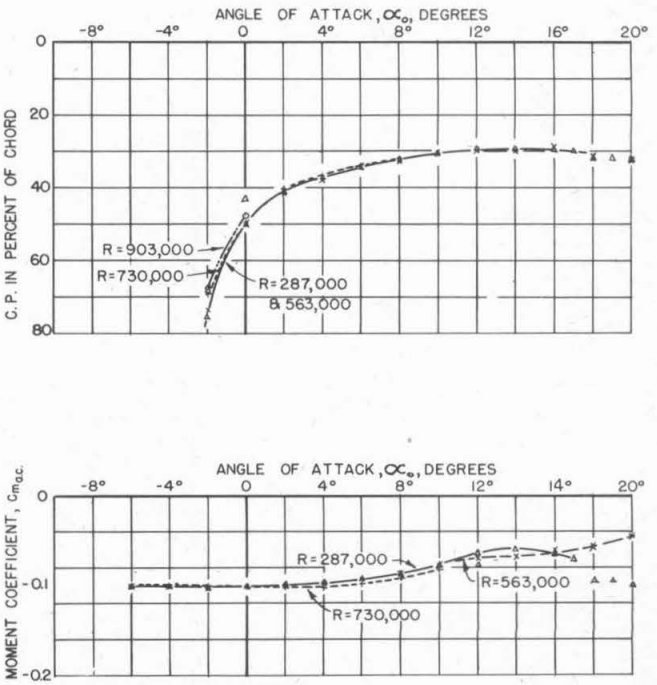

Fig. 17.

Infinite Aspect Ratio Characteristics vs. Angle of Attack

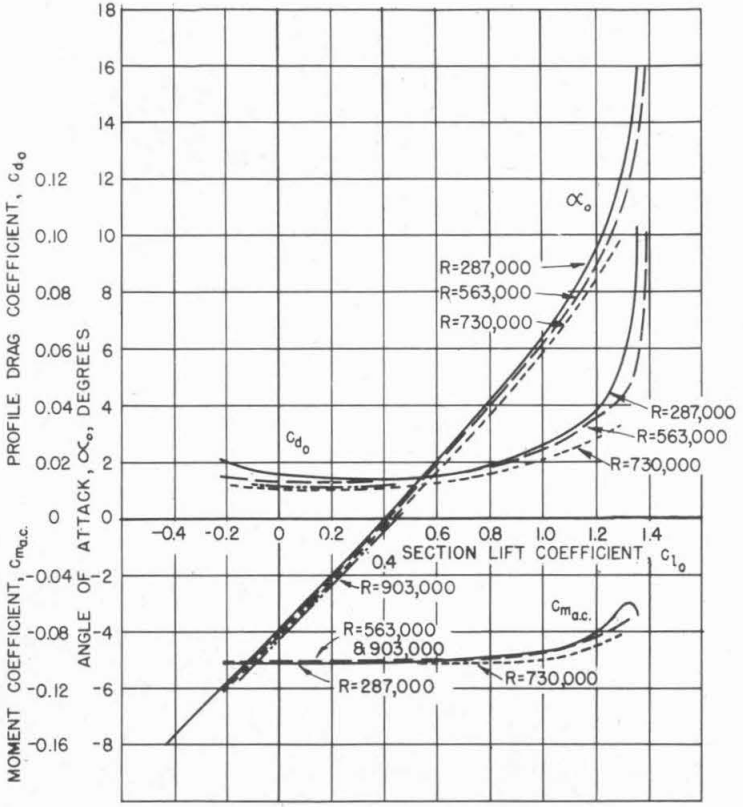

Fig. 18.

Infinite Aspect Ratio Characteristics vs. Lift. Coefficient

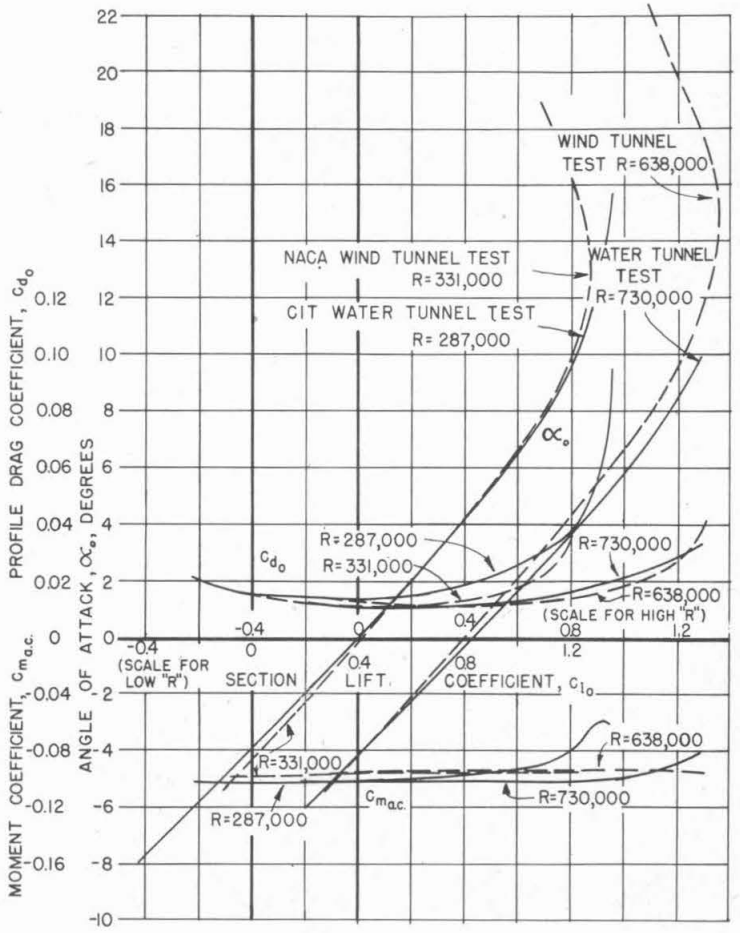

Fig. 19.

Comparison of Water Tunnel Results with Wind Tunnel Data from Tests on a Finite Span Unit of Aspect Ratio Six